

SYMPOSIUM ON PYROLYSIS REACTIONS OF FOSSIL FUELS  
PRESENTED BEFORE THE DIVISION OF PETROLEUM CHEMISTRY, INC.  
AMERICAN CHEMICAL SOCIETY  
PITTSBURGH MEETING, MARCH 23-26, 1966

ON THE KINETICS OF CO AND CH<sub>4</sub> FORMATION DURING COAL PYROLYSIS  
AT TEMPERATURES IN THE RANGE 570° - 670°C\*

By

W. J. Mullin and N. Berkowitz  
Research Council of Alberta  
Edmonton, Canada

Following two earlier kinetic studies in which we directed attention to the formation (or, more correctly, the disengagement) of elemental hydrogen and water in the temperature interval between 650° and 850°C (1, 2), we deemed it of some interest to extend the investigations to methane and carbon monoxide which, together with hydrogen, are the principal products discharging from a coal char between 550° and 700°C. This paper reports our findings.

Pending completion of an ancillary study which was suggested by the work here described (an initiated while it was still in progress), we think it inappropriate to offer more than a tentative generalized interpretation of the experimental results. But we would observe that the data obtained in the course of the present investigation are in broad accord with earlier ones in again stressing the role of diffusional processes as rate-controlling mechanisms. Unless coupled with more discriminating methods of experimentation, formal kinetic studies seem to us therefore increasingly unlikely to yield significant information about the chemical transformations associated with coal carbonization.

#### EXPERIMENTAL

Though somewhat refined in matters of detail, the experimental methods used in this study were essentially those employed in the previous investigations (1, 2), i. e., test samples were first vacuum-carbonized at 550°C in order to free them from all tarry material and then heated in helium to a pre-selected temperature which was maintained for a sufficiently long period to permit completion of an appropriate gas sampling and evaluation program. Gas samples were in all cases analyzed by gas chromatographic techniques which also allowed automatic recording of gas discharge rates.

The apparatus in which initial carbonization and, later, the kinetic measurements were performed is shown in diagrammatic form in Figure 1 and consisted of an electrically-heated tube-furnace connected to a vacuum system and a suitable g. c. assembly. The latter comprised a gas sampling cell (shown in the diagram) coupled to a 7-ft. long, 1/4 inch dia. column of -42 +60 mesh 13X Linde molecular sieve, a Gow-Mac thermal conductivity cell, and a variable-speed Fisher recorder.

Temperature control was exercised by a Pt-Pt/10% Rh thermocouple whose hot junction was located within the furnace tube, immediately adjacent to the sample holder. The cold junction leads connected with a Beck pulse-time modulation program control unit and a recorder.

To carry out a run, ca. 1 gm. of dry < 48 mesh coal (see below) was placed in a small, open-ended tared quartz tube, and the tube loosely plugged with asbestos, weighed and inserted into the furnace tube. The entire assembly was then repeatedly flushed with dry helium and slowly evacuated for several hours, after which the coal was gradually raised to 550°C and there held for 90 minutes. Throughout this time, a good vacuum was maintained and care was taken to ensure a positive pressure of helium in all non-evacuated lead-lines to the furnace.

When degassing was complete, helium was slowly admitted to the system until atmospheric pressure was restored, the helium flow adjusted to 60 ml. min<sup>-1</sup> and the furnace tube switched to connect with the g. c. sampling and detection assembly. Thereafter, the furnace was re-set for, and quickly raised to, the required experimental temperature in the range 570°-670°C. The re-set time represented the experimental "zero point". During heat-up and at the final temperature, gas samples were routinely taken and analyzed at three-minute intervals until gas discharge rates from the char were so small as to be virtually undetectable. When this point had

\*Contribution No. 322 from the Research Council of Alberta.

been reached, the power supply was interrupted, the furnace allowed to cool to room temperature, and the sample then removed and re-weighed. Comparison of the char weight loss thus established with a previously constructed w/T curve permitted mass balances to be worked out and also allowed expression of gas yields on a "per gm. 550°C char" basis.

In order to obtain sufficiently detailed data for kinetic evaluation, at least three separate test runs were carried out at each temperature and the gas sampling program so arranged as to overlap. Thus, if in the first run sampling began one minute after "re-set", it was started 2 minutes after "re-set" in the second, and 3 minutes after "re-set" in the third. Figure 2 illustrates this procedure (and the close agreement between data from the different runs) with a composite rate curve representing a complete set.

Initial calibration of the g. c. column and detector was carried out in the usual manner by means of several, carefully prepared CH<sub>4</sub>/CO/He mixtures; but in addition, routine calibration checks were also made after each completed set of runs.

To explore the effect of coal type, discharge rates from the three widely different coals were examined. These were (a) a semi-anthracite from the Cascade area of SW Alberta (designated as #1); (b) a bituminous coking coal from the Crownsnest Pass region (designated as #2); and (c) a subbituminous coal from the Drumheller field of C. Alberta (designated as #3). Prior to carbonization, these coals were crushed to < 48 mesh, flotation-cleaned at s. g. = 1.35, extracted with 10% HCl, and finally washed with distilled water and vacuum-dried. The prepared samples were stored under purified nitrogen in gas-tight bottles. Table 1 lists their relevant analytical parameters.

TABLE 1

Coal	Ash, %	Carbon %	d. a. f.		
			Hydrogen %	Sulfur %	Oxygen %
#1	2.33	89.4	4.1	0.7	5.8
#2	4.96	86.8	5.1	0.7	7.4
#3	5.99	73.3	4.8	0.5	21.4

#### DATA PROCESSING

Conversion of the raw data--i. e., of the chromatograms traced by the recorder--into the forms necessary for kinetic analysis was achieved by a series of individually very simple transforms. In step I, recorded peak heights were changed into areas; where necessary, corrected for attenuation during measurement of discharge rates; and finally recalculated to STP gas volumes gm<sup>-1</sup> of 550°C char. Figure 2 shows a typical rate curve thus obtained. In step II, the rate curves were graphically integrated; cumulative yields (y) to various reaction times (t) plotted as functions of t; and the resultant plots transcribed to punched tape which could be computer-extrapolated to t = ∞ to give the total yield (y<sub>0</sub>) of CO or CH<sub>4</sub> obtainable at each temperature (T). Plots of y versus ln t were used to estimate the theoretical zero time point and to correct for the non-instantaneous approach to the reaction temperature. (Figure 3 illustrates the procedure.) Finally, in step III, cumulative yields were normalized to take account of the fact that y<sub>0</sub> itself varies with T, and appropriate functions of y/y<sub>0</sub> plotted against t to establish the apparent order of the reaction. For a pseudo-first order--which had been found for the disengagement of hydrogen (1) and water (2)--this meant graphing -ln(1-y/y<sub>0</sub>) against t.

#### RESULTS AND DISCUSSION

The sequence of diagrams reproduced in the following pages summarize the results obtained in this manner. In each diagram, empty circles (○) denote data relating to coal #1, while ● and ⊙ refer, respectively, to coals #2 and #3.

The variation of cumulative yields (y) of methane and carbon monoxide with time (t) at constant temperature (T) is illustrated in Figures 4 and 5 which, near their right hand margins, also contain the estimated final yields (y<sub>0</sub>) of CH<sub>4</sub> and CO at each temperature. Figures 6 and 7 show these latter quantities as direct functions of T.

Figures 4 and 5 are, in themselves, quite unremarkable and are here merely placed on record. But some interest attaches to the observation (cf. Figure 6) that over the temperature

interval covered by this study,  $y_0(\text{CO})$  is for all practical purposes a linear function of  $T$  whose slope is proportional to the oxygen content of the parent (550°C) char. By contrast,  $y_0(\text{CH}_4)/T$  assumes a more familiar sigmoid form--although there is, even in this case, a suggestive differentiation between coal #1 on the one hand and coals #2 and #3 on the other. We refer, in particular, to the variation of  $y_0(\text{CH}_4)$  with  $T$  at  $T < 600^\circ\text{C}$  (cf Figure 7).

These matters, however, are of less immediate interest than the information offered by kinetic treatment of the experimental data. As shown in Figures 8-10 (for CO) and 11-13 (for  $\text{CH}_4$ ), test plots of  $-\ln(1-y/y_0)$  vs.  $t$  indicate not only general conformity to pseudo-first order kinetics, but also suggest the possibility that rates of CO and  $\text{CH}_4$  disengagement at temperatures in excess of ca. 600°C may be controlled by at least two mechanisms: in all instances,  $-\ln(1-y/y_0)/t$  exhibits a fairly sudden change of slope above some value of  $y/y_0$ , though the point at which this discontinuity occurs appears to vary quite regularly with temperature. Table 2 will serve to illustrate this.

TABLE 2

Coal	Temperature, °C	$y/y_0(\text{CO})$ at "break"	$y/y_0(\text{CH}_4)$ at "break"
#1	612	0.245	0.25
	645	0.525	0.59
	668	0.535	0.675
#2	603	0.28	0.26
	634	0.39	0.51
	663	0.48	0.635
#3	612	0.26	0.31
	641	0.455	0.45
	673	0.60	0.64

The possibility that behavior above the discontinuity in the  $-\ln(1-y/y_0)/t$  plot merely connotes some unspecified departure from the norm cannot, perhaps, be dismissed out of hand. And apparent activation energies ( $E$ ), calculated on that assumption from the initial slopes of each set of  $-\ln(1-y/y_0)$  vs.  $t$  plots would then suggest that rates of CO and  $\text{CH}_4$  disengagement are controlled by processes formally akin to activated diffusion (cf. Table 3).

TABLE 3

Coal	Temperature Range °C	CO Disengagement $E$ , kcal mole <sup>-1</sup>	$\text{CH}_4$ Disengagement $E$ , kcal mole <sup>-1</sup>
#1	577 - 668	10.1	15.7
#2	577 - 664	7.9	16.5
#3	576 - 673	14.5	17.0

However, bearing in mind the consistently linear variation of  $-\ln(1-y/y_0)$  with  $t$  above as well as below the "break", it seems fundamentally more reasonable to regard the initial slopes as composites of two superimposed reaction sequences and to resolve them in the manner illustrated in the diagrams (cf. Figures 8-13). The straight lines there designated by the velocity constant  $k_1$  (and drawn to parallel  $-\ln(1-y/y_0)/t$  above the "break") reflect one reaction or control mechanism, while those characterized by  $k_2$  (and drawn as the vertical difference between  $k_1$  and the observed rate) indicate the other. That reactions designated by  $k_2$  should in all instances terminate fairly abruptly follows from the form of the discontinuity in the experimental  $-\ln(1-y/y_0)/t$  plots.

Apparent activation energies computed on this basis are set out in Table 4 and establish a marked dichotomy. While values of  $E$  calculated via  $k_1$  are consistently less than 5 kcal mole<sup>-1</sup> (and therefore indicative of simple diffusion control over  $k_2$ ), those obtained via  $k_2$  are almost large enough to connote some chemical (i. e., reaction) control. They are, in any event, the highest values so far recorded in these laboratories.

TABLE 4

Coal	CO Disengagement		CH <sub>4</sub> Disengagement	
	E via $k_1$ kcal mole <sup>-1</sup>	E via $k_2$ kcal mole <sup>-1</sup>	E via $k_1$ kcal mole <sup>-1</sup>	E via $k_2$ kcal mole <sup>-1</sup>
#1	2.5	35.1	1.7	55.2
#2	0.5	33.5	3.3	38.1
#3	3.6	22.6	4.4	38.5

Pending completion of a study now in progress, we prefer (as already indicated) to reserve comment on these findings. But it is important to observe that the data in Table 4 do not necessarily imply the operation of two distinctly different rate control mechanisms and that they can, in fact, be more easily and adequately accounted for by several models which only presuppose differential diffusion.

Qualitatively, this is perhaps most conveniently illustrated by considering a structurally isotropic, porous sphere which, at a given temperature  $T$ , suffers partial thermal decomposition and thus forms a quantity of gas which derives uniformly from every volume element of the sphere (i. e.,  $(\partial g / \partial v)_T = \text{constant}$ ). For the greater part, escape of this gas will be impeded by internal geometry and consequently diffusion-controlled. Superimposed upon this, however, there will also be a substantial quantity of gas which originates in near-surface volume elements and can therefore discharge at rates essentially equal to those at which it forms. And there will be some gas which can disengage from the char at rates intermediate between these two "extremes".

Several restrictions must, of course, be placed upon such a model in order to make it quantitatively conform with the experimental results, and we are currently exploring these in some detail. It is, however, significant that even a generalized model seems capable of accounting for the observation that the "break" in  $-\ln(1-y/y_0)/t$  occurs at progressively higher values of  $y/y_0$  as  $T$  increases: we note that this would follow from the pronounced temperature-dependence of  $y_0$  and from the relative volumes of near-surface and core elements of a sphere.

#### LITERATURE CITED

- (1) Berkowitz, N., and den Hertog, W.; *Fuel*, **41**, 507, 1962.
- (2) Neufeld, L. F., and Berkowitz, N.; *ibid.*, **43**, 189, 1964.

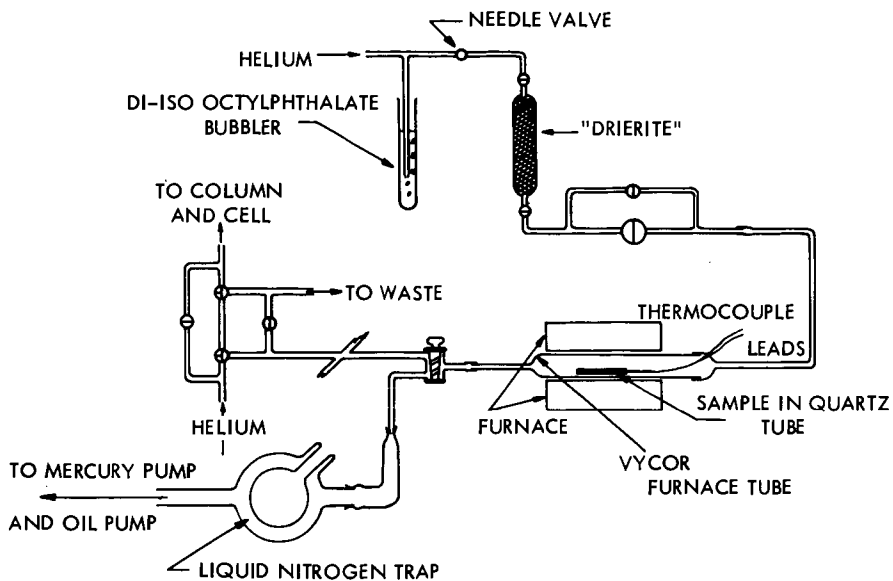
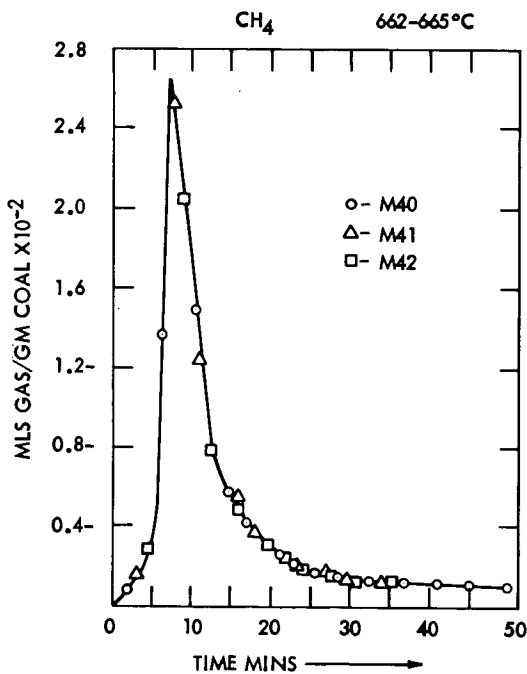
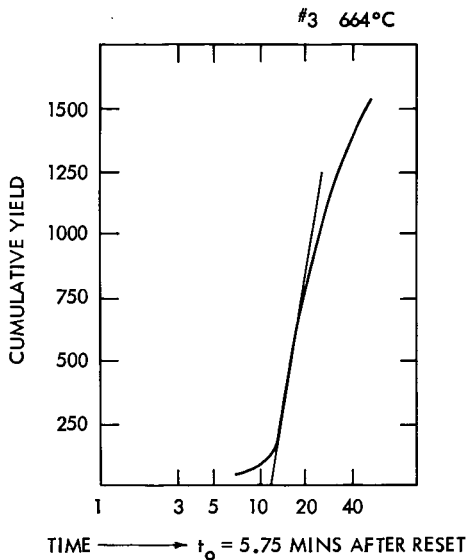


DIAGRAM OF APPARATUS

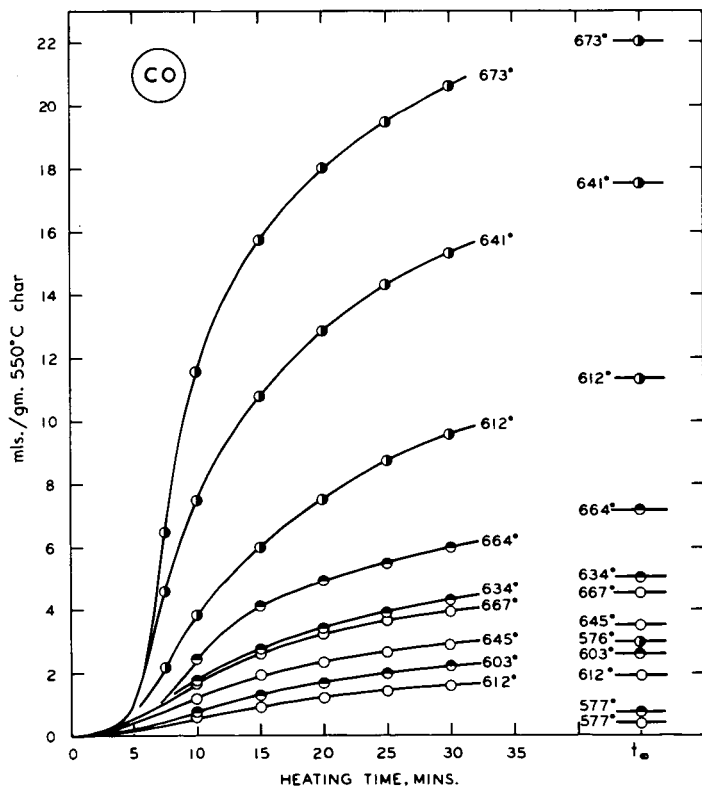
(1)



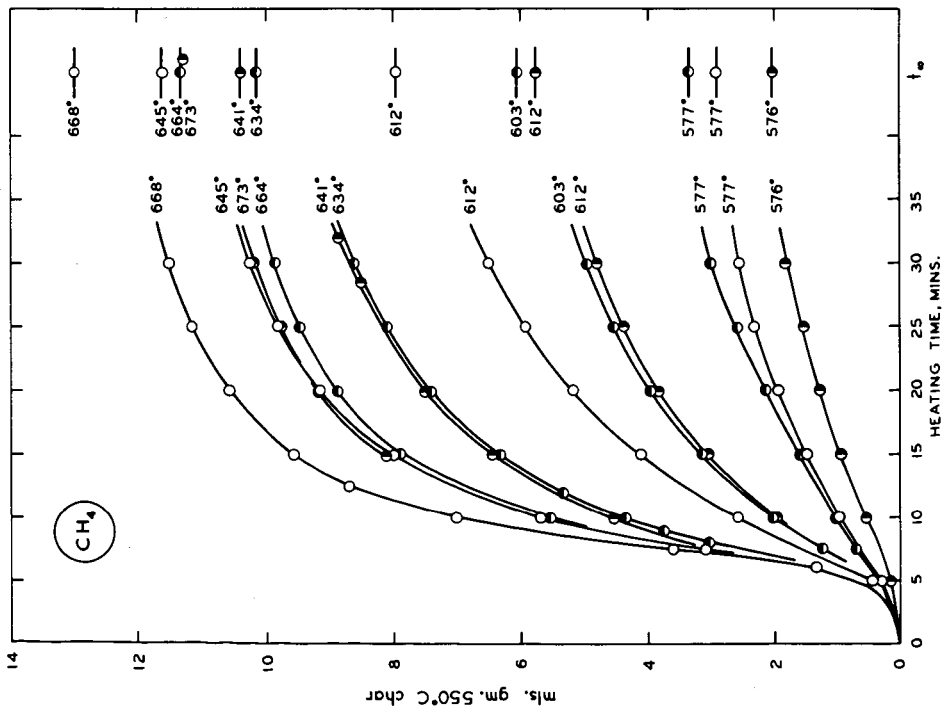
(2)



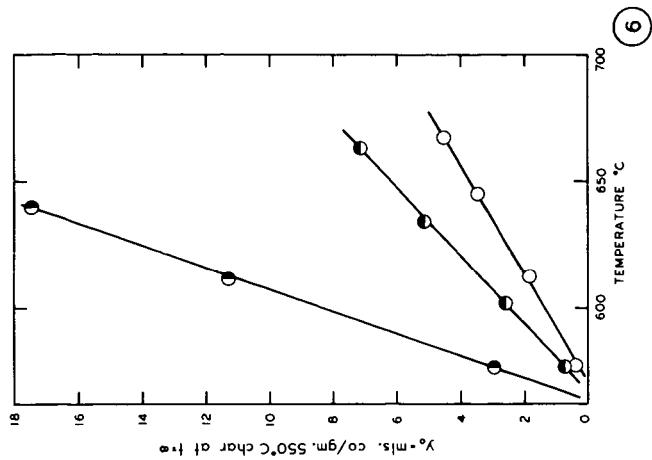
3



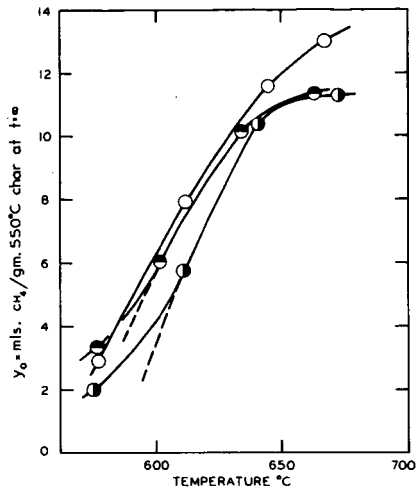
4



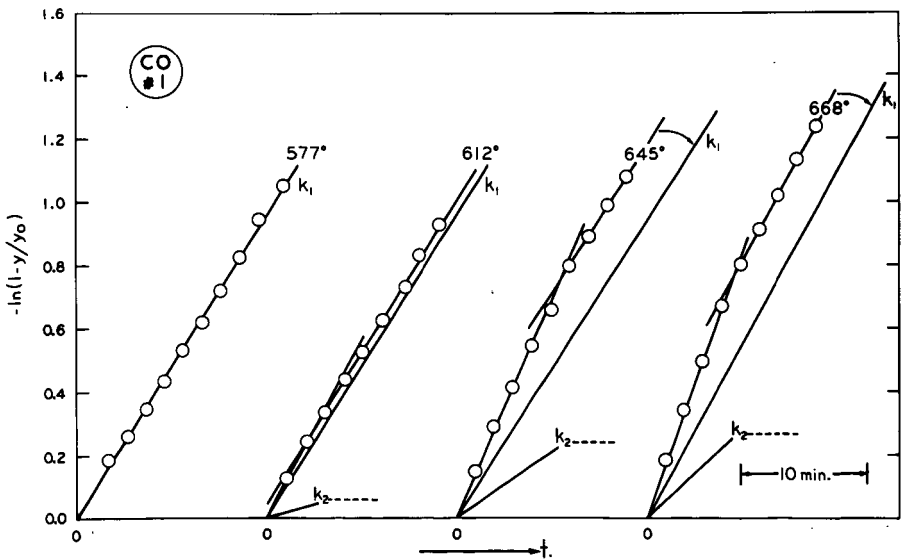
5



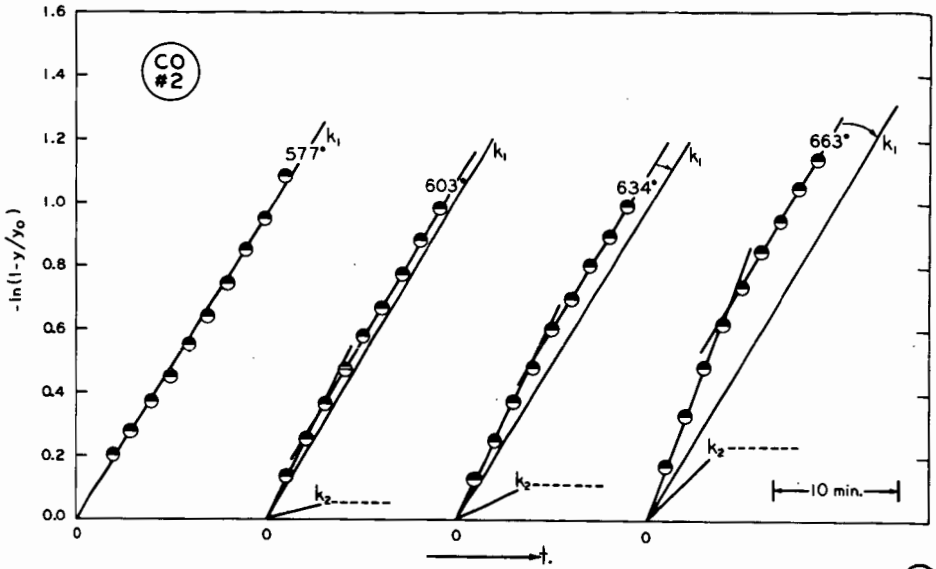
6



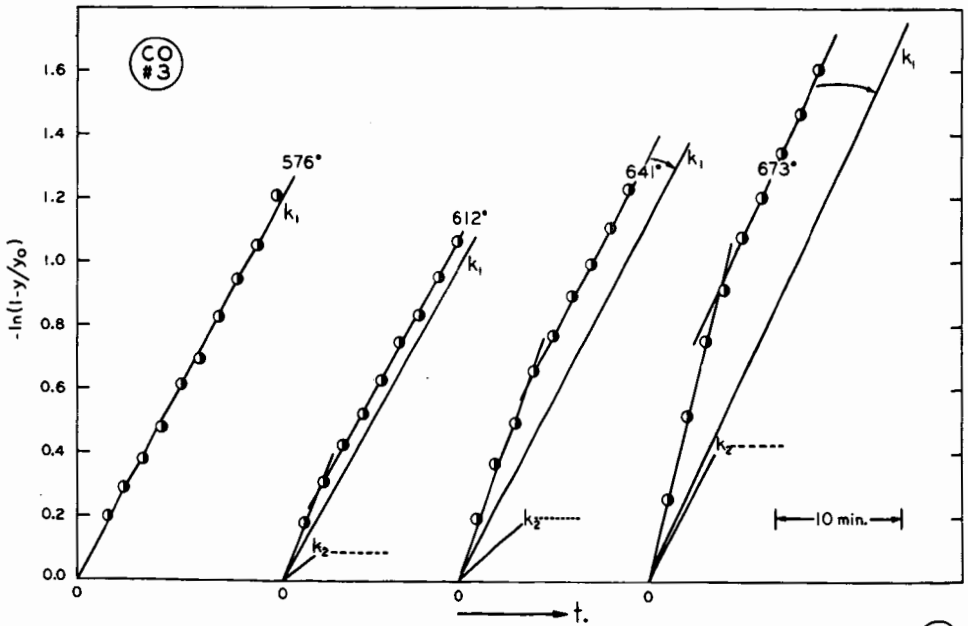
(7)



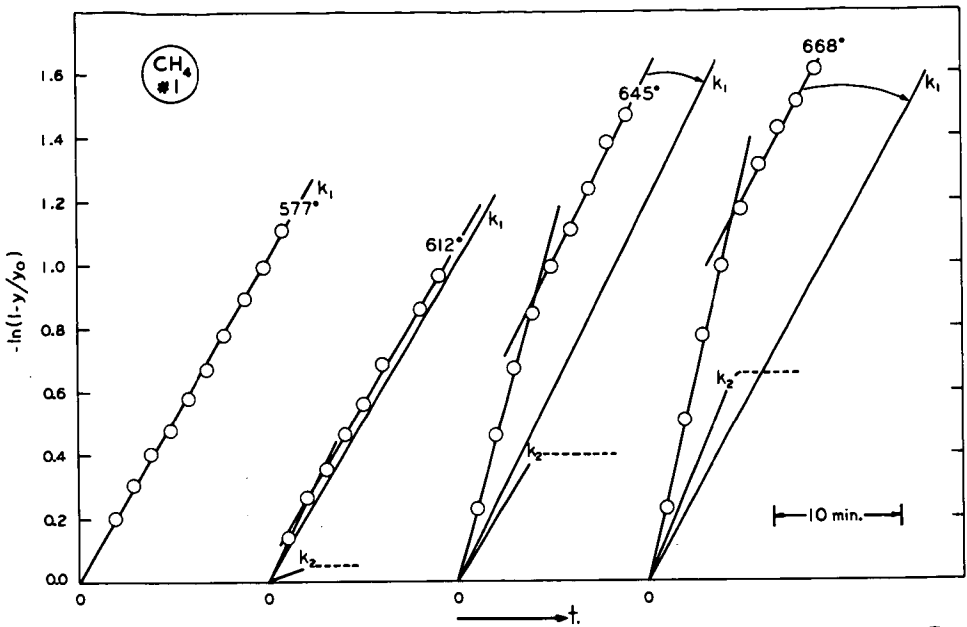
(8)



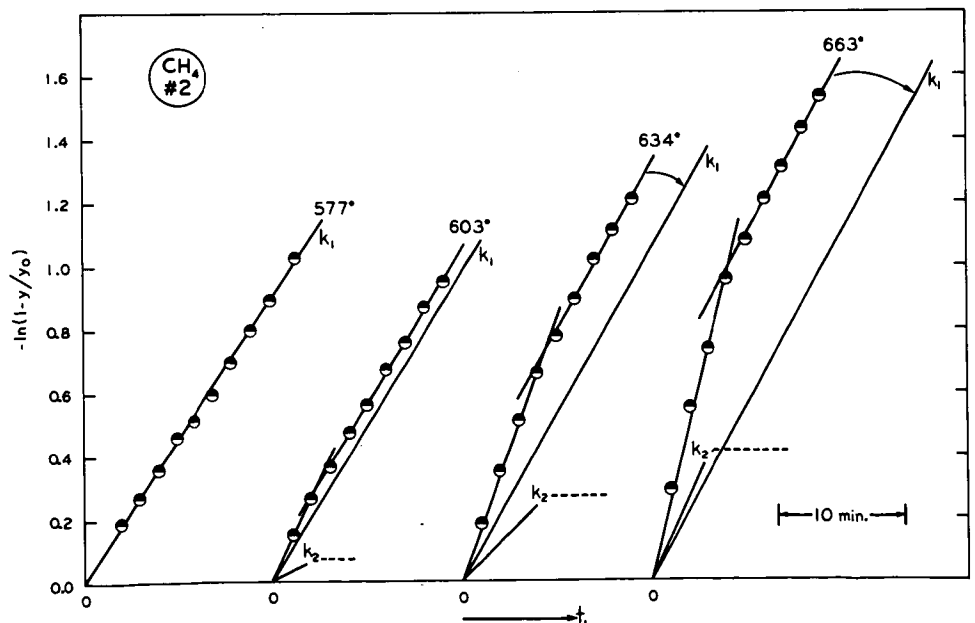
9



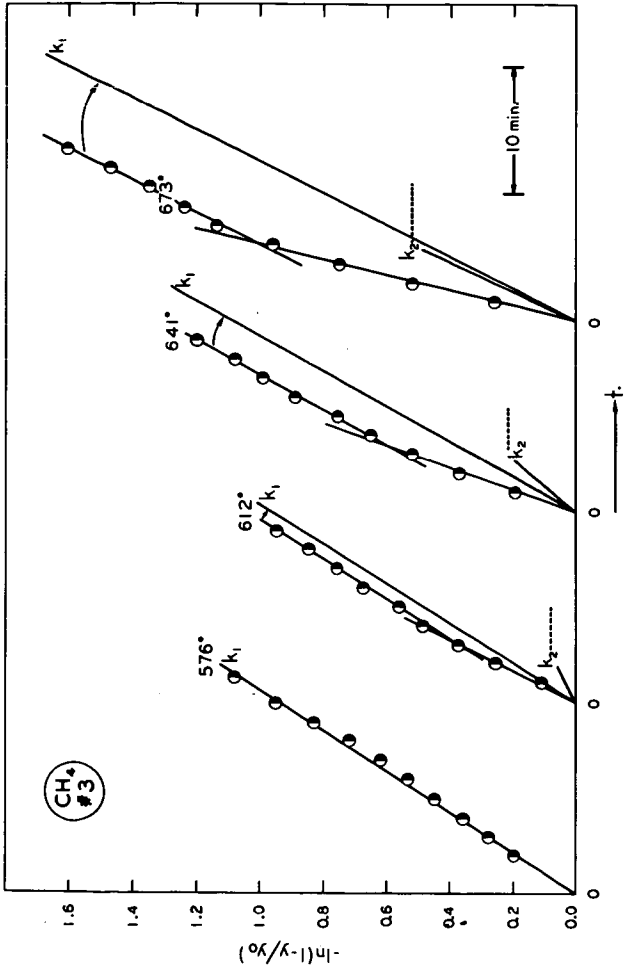
10



11



12



(13)